Vibrational Stark Effects on Carbonyl, Nitrile, and Nitrosyl Compounds Including Heme Ligands, CO, CN, and NO, Studied with Density Functional Theory

Sergio D. Dalosto,[†] Jane M. Vanderkooi, and Kim A. Sharp*

Johnson Research Foundation, Department of Biochemistry and Biophysics, School of Medicine, University of Pennsylvania, Philadelphia, Pennsylvania 19104

Received: September 16, 2003

Changes in the matrix electric field in a protein, due for example to mutations or structural fluctuations, can be correlated with changes in the vibrational transition frequencies of suitable chromophores measured by IR spectroscopy through the Stark tuning rate. To make this correlation, the Stark tuning rate must be known from experiment or theory. In this paper, density functional theory at the B3LYP/TZV level of theory is used to compute the Stark tuning rate of adducts of heme porphyrin, namely, −CO, −CN, and $-NO^+$ compounds. The results are compared with the corresponding vibrational frequencies−field dependencies from vibrational Stark spectroscopy of heme−proteins. The zero-field computed Stark tuning rate of 1.3 cm^{-1}/MV/cm for heme−CO is in agreement with experiment, where typically the rate is $2.4/f$ cm^{-1}/MV/cm for myoglobin, where f is a local field correction between 1.1 and 1.4. Several small nitrile, carbonyl, and dinitrile molecules were studied to rationalize the findings for the heme-adducted models. Here, the higher B3LYP/6-311++G-(2d,2p) level of theory could be used so the agreement with recent experimental results is even better than for heme-adducted groups.

Introduction

In nature, many thousands of types of proteins exist, each with unique structure. The packing of the 20 amino acid residues that make up these proteins plays a fundamental role in determining structure and function, but reactivity, dynamics, and folding specificity of the protein are ultimately also decided by electrostatic interactions between groups. Insight into electrostatic interactions can be obtained by considering how the transition energy of a chromophore is influenced by electric fields. The shift of a particular transition is dependent upon the transition dipole moment of the chromophore and its polarizability. The change in the wavenumber of absorption due to the electric field is called the Stark effect. The imposed field can be externally applied or can arise from the local field imposed by neighboring groups in the protein. The latter phenomenon is called an internal Stark effect.

A Stark effect can be seen for all types of spectroscopy. The effect of the protein field has been experimentally studied for the optical spectra of sensitive probes such as tyrosine,[1,2] tryptophan,[3] redox chromophores in proteins[4−7] recently Aladan,[8] or nitrile-derivatized amino acids.[9] The shift is determined by the electronic structure of the group and the local field at the group. With IR spectra, the influence of fields can be examined at effectively atomic resolution and at defined locations of interest within the protein. The experimental way to correlate a shift in frequency with the electric field is to observe a shift when an external electric field is applied, in the technique called vibrational Stark effect (VSE) spectroscopy. From the VSE, it is possible to infer the Stark tuning rate, $\Delta\mu$, the frequency shift for a particular group as a function of field.[10] The ideal group to probe the environment and the structure of specific sites in proteins would be one that has IR absorbance bands in a spectral region that is separate from other absorbing groups. This condition is met by three groups currently being used for Stark measurements: −CO (carbonyl),[11] −CN (nitrile),[12−15] and −NO (nitrosyl).[16]

A requirement for the use of VSE is that we understand the underlying physical theory. The Stark tuning rate is not necessarily linear with applied field nor is the effect symmetrical around a particular group.[17] Furthermore, an IR band may be the combination of several vibrational modes, and therefore to understand one mode of vibration, we need to do a quantum calculation that considers the whole molecule. It is also necessary to understand under what conditions, and by how much, the Stark tuning rate measured by external VSE may be altered in a particular protein to correctly extract fields from frequency shifts. Understanding these factors will help in the selection of suitable functional groups for use in VSE experiments. The role of the protein matrix in influencing prosthetic groups through electrostatic interactions is probably the most complex of the factors to understand due to the large number of atoms in the protein. However this is a subject that is becoming increasingly amenable to study by computational methods. The goal of this paper is to show that it is possible to calculate the tuning rate in advance of experiment, both for small compounds and protein systems, with the view of both interpreting existing experiments and making predictions for future experiments.

Methods and Theory

The goal is to calculate changes in the vibrational frequency of a molecule due to an external electric field, F. The VSE can be quantified by the Stark tuning rate, $\Delta\mu_{\nu F} = (d\nu/dF)_{F=0}$.[18] Different approaches have been used to calculate $\Delta\mu_{\nu F}$, com-

* To whom correspondence should be addressed. E-mail: sharpk@mail.med.upenn.edu.

[†] Present address: Yale University, Department of Chemistry, P.O. Box 208107, New Haven, CT 06520-8107.

10.1021/jp0310697 CCC: $27.50
Published on Web 04/24/2004

TABLE 1: Effect of Basis Sets Used on the Calculated Stark Tuning Rate for ν_{CN} in 4-Chloro-benzonitrile

	basis sets	$\Delta\mu_-$	$\langle\Delta\mu\rangle$	$\Delta\mu_+$
1	6-31G	0.371	0.465	0.56
2	6-31G(d)	0.292	0.394	0.497
3	6-31G(d,p)	0.294	0.395	0.496
4	6-31+G(d)	0.397	0.513	0.630
5	6-31++G	0.37	0.58	0.62
6	6-31++G(d)	0.38	0.51	0.64
7	6-311G(d)	0.30	0.435	0.57
8	6-311G(d,p)	0.30	0.435	0.57
9	6-311++G(2d,2p)	0.42	0.504	0.59

bining experimental information with the expansion of the energy in terms of F and some relevant distance.[19−21] It is possible to model free small molecules such as, e.g., CO adducted on a metal surface by combining experimental information with the expansion of the energy.[22,23] Numerous studies used perturbational theory[24] or expansion in a Taylor series in terms of F and a relevant distance (i.e., the CO distance).[20] Ab initio or DFT[15,25] calculations of $\Delta\mu_{\nu F}$ have proven successful and complementary to analytic methods. In this work, we used density functional theory (DFT) methods to evaluate the tuning rate.

Computational Methods

DFT Calculations. Three different exchange-correlation functionals were used to evaluate the effect of the electric field in the stretching frequencies of the heme adduct. The first was Becke's three-parameter hybrid functional with the correlation functional of Lee, Yang, and Parr (B3-LYP).[26−28] The second one was Barone's and Adamo's Becke-style one-parameter functional using a modified Perdew−Wang exchange and Perdew−Wang 91 correlation (PW91).[29] The third exchange correlation was the Xα with the correlation functional of LYP and $\rho = 0.7$. All the calculations were performed using the standard options in the Gaussian 98 program package.[30] The basis sets used for the heme adduct were 6-31 G, 6-311+G-(d,p), and TZV.[31] For the small molecules such as CO, CN^-, HCN, CNH, NO, acetone, 1-methyl-2-pyrrolidinone, acetonitrile, 4-chloro-benzonitrile, benzonitrile, and 1,4-dicyano-2-butene, we used the B3LYP functional and the basis 6-311++G(2d,2p).

The uniform electric field was explicitly included in the optimization and in the frequency calculation of every molecule studied in this paper. The first step was to optimize the molecule in the presence of an external and uniform electric field. After the full molecular optimization, we used that relaxed structure, and in the presence of the same electric field, we calculated the stretching frequency. The direction of the electric field was set parallel to the bond Fe → C → N in the heme models or parallel to C → N/O for the small molecules. The geometry optimization and the stretching frequency were computed using analytic gradients.[30] For example, in the notation Fe → C → N, the arrows indicate the direction of the electric field going from positive to negative, the corresponding frequency is ν_+, when the electric field is going from negative to positive, Fe ← C ← N, the frequency is called ν_-. The electric field values used were 0.0, ±0.005, and ±0.01 au (1 au ≡ 5.14225 GV cm^{-1}). The range of electric fields was selected considering the estimated fields imposed by the close groups in protein, as found in the citations above.[10−15] All the frequencies tabulated in Tables 2 and 3 are given without scaling. The vibrational tuning rate for each model studied was computed taking the slope in the limit when the electric field goes to zero, making use of the best polynomial that fit the frequency vs electric field to determine the zero value.

Heme Models. We studied several different kinds of clusters. These clusters were Fe−porphine−CO ($FeC_{25}H_{18}N_6O$) or Fe−porphine−NO^+ ($FeC_{24}H_{18}N_7O$) and Fe−$N_{pyridine}$−XY, where XY can be CO or CN with the stoichiometry $FeC_{12}H_{15}N_5O$ or $FeC_{12}H_{15}N_6$, respectively. In Fe−porphine−CO, the proximal histidine was modeled by imidazole−CH_3. Imidazole was used to model the proximal histidine in Fe−porphine−NO^+. In Fe−$N_{pyridine}$−XY, the proximal ligand is the symmetric pyridine; both models were used successfully in previous studies.[32,33] Figure 1 shows the models used to study the effect of the electric field. For the adducted −CO, the oxidation state of iron is ferrous, and the spin state is $S = 0$ with total charge zero. For −CN adducts, we studied two models. One was ferric with $S = {}^1/_2$ and charge zero, and the other was ferrous with spin 0 and charge −1. For $-NO^+$, we used the spin $S = 0$ and charge $q = +1$.

Results

Examination of the Choice of the Basis Set for One Molecule. We studied the effect of the basis sets in the tuning rate and frequency for the model compound 4-chloro-benzonitrile. The basis sets used are listed in Table 1 together with the calculated tuning rates. The tuning rates, in this case, were computed by taking the slope $\Delta\mu_+ = (\nu_0 - \nu_+)/F$ or $\Delta\mu_- = (\nu_- - \nu_0)/F$, $\langle\Delta\mu\rangle = (\Delta\mu_+ + \Delta\mu_-)/2$, where ν_+, ν_-, and ν_0 are the frequencies of the CN stretching normal mode with the electric field positive, negative, and zero. This procedure allows us to evaluate the asymmetry with respect to the direction of the applied electric field. The applied electric field was $F = 0$ and ±0.005 au. The experimental tuning rate of 4-chloro-benzonitrile[13,12] is $0.58/f$, where f is a local-field correction factor between 1.1 and 1.4.[34] The effect of the correction factor would mean that the tuning rate would be between 0.53 and 0.41. Except for basis sets 6−31 G(d) and 6-31G(d,p), the rest give good agreement within the interval of uncertainty of the local-field correction factor. The use of polarization (d,p) and diffusive (+) functions should be more important when the sensitive nitrile probe is inside a protein interacting with neighboring residues.

Field-Dependent Frequency and Geometries of Small Molecules. Electric field effects on small molecules containing the CO or CN groups were carried out in order to have a reference and to compare with numerous studies in the literature. Table 2 shows the calculated tuning rate for small molecules. The last column of Table 2 also shows computed values from a recent paper of Brewer and Franzen.[25] The agreement between computation and experiment is in general good for both computations. We note that the computations were carried out in vacuum, whereas the experiments are always carried out in solvent, for example, tetrahydrofuran with a dielectric constant $\epsilon \approx 8$. Specific solvent−solvent and solvent−solute forces should be considered to explain the small difference between calculated and experimental values. This issue was addressed by Reimers and Hall in ref 35.

Small carbonyl molecules such as acetone have tuning rates similar to free CO: $0.75/f$ and $0.61/f$ cm^{-1}/MV/cm, respectively.[11] For 1-methyl-2-pyrrolidinone, the experimental tuning rate is a bit greater: $1.14/f$ cm^{-1}/MV/cm. In this particular case, the calculations underestimated the experimental value beyond the interval defined by the correction factor f. The estimated ratio is $|\Delta\mu|^{exp}/|\Delta\mu|^{theo} \approx 1.7$, see last column of Table 2.

Stark tuning rates were next calculated for CN^- and small nitrile molecules, 4-chloro-benzonitrile and 1,4-dicyano-2-butene have experimental values for Stark tuning rates of $\Delta\mu = 0.58/f$

TABLE 2: Calculated and Observed Vibrational Stark Effect on CO and Nitrile Stretch for Small Molecules[a]

	ν (cm^{-1})		$\lvert\Delta\mu\rvert$ (cm^{-1}/MV/cm)			
			calc this work			
	exp	calc this work	exp	$\lim_{F\to 0}$	$\lvert\Delta\mu\rvert^{exp}/\lvert\Delta\mu\rvert^{theo}$	$\lvert\Delta\mu\rvert$, ref 25
CO	2130	2209	0.67	0.51	1.3	0.467
acetone	1711	1779	0.75	0.58	1.3	0.690
1-methyl-2-pyrrolidinone	1685	1675.3	1.14	0.69	1.7	
CN^- ($q=-1$, $S=0$)	2080.6	2124		0.16		0.223
CNH ($q=0$, $S=0$)		2099		0.8		
HCN ($q=0$, $S=0$)	2072	2193		0.05		0.098
acetonitrile	2247.5	2315	0.43	0.26	1.6	
4-chloro-benzonitrile	2230.6	2322	0.58	0.50	1.2	0.680
benzonitrile	2227.8	2261		0.44		
1,4-dicyano-2-butene	2251.3	2350[b]	0.31	0.33[b]		
NO ($q=0$, $S=1/2$)		1957		0.36		
NO^+ ($q=+1$, $S=0$)		2465		0.25		

[a] Experimental information was taken from Park and Boxer.[11] All the calculated frequencies are without scaling. [b] See text. Because of the symmetry of this molecule, there are two modes of vibration, symmetric (S) and antisymmetric (A), the S is 50 times more intense than the A (this work). The average shift in frequency of the S mode with $F=\pm 0.01$ au (± 51.4225 MV/cm) is ~ 22.2 cm^{-1} with respect to the value with the field off. The $\Delta\mu$ was computed using this shift.

TABLE 3: Calculated Frequencies at Three Fields and Vibrational Stark Effect of −CO, −CN, and −NO in Heme Models and Comparison with Experimental Results

calculations			field for calculation (MV/cm)			Cal$Lim_{F\to 0}$	experiments	
adduct	model and basis	method	−51.14 cm^{-1}	0 cm^{-1}	+51.14 cm^{-1}	$\lvert\Delta\mu\rvert$ (cm^{-1}/MV/-cm)	ν (cm^{-1})	$\lvert\Delta\mu\rvert$ (cm^{-1}/MV/-cm)
−CO ($q=0$, $S=0$)	Fe−Porphine−CO TZV	B3LYP	1982	1917	1849	1.3	1900−1970[a]	2.3
	Fe−Porphine−CO 6-31G	B3LYP				1.2		
	Fe−$N_{pyridine}$−CO TZV	PW91				1.3		
	Fe−$N_{pyridine}$−CO 6-31G	B3LYP				1.2		
	Fe−$N_{pyridine}$−CO 6-311+G(d,p)	B3LYP				1.33		
−NO ($q=0$, $S=1$)							1917−1904[b]	2.0
$-NO^+$ ($q=+1$, $S=0$)	Fe−Porphine−NO^+	B3LYP	1953	1921	1855	0.84		
−CN ($q=0$, $S=1/2$ ferric)	Fe−$N_{pyridine}$−CN	B3LYP	2165	2150	2119	0.45	2130[c]	ND[d]
−CN ($q=-1$, $S=0$ ferrous)	Fe−$N_{pyridine}$−CN	B3LYP	2125	2087	2034	0.88	2029−2057[c]	ND
−CNH ($q=0$, $S=0$)	Fe−$N_{pyridine}$−CN	B3LYP	2085	2024	1875	2.0		ND

[a] Different Mb−CO mutants. A complete list is available in ref 48. [b] Reference 10. [c] References 49 and 46. [d] ND = no data available.

and $0.31/f$ cm^{-1}/MV/cm, respectively. Again, the agreement with experiment is reasonable (Table 2). From the point of view of future experiments, it is noteworthy that the calculated tuning rate of the isocyanide CNH is relatively high. A recent review of its importance in organoisocyanides can be found in ref 36.

To our knowledge, an experimental tuning rate is not available for free NO or NO^+ nor has it been theoretically calculated. Our calculated values predict a smaller field effect for NO than for CO. The NO field effect is greater than for HCN or CN^- (Table 2). The consequence of the small field effect for HCN and CN^- will mean that the detection of the Stark effect would be difficult for these groups.

Changes of Stretching Frequency ν_{CN} with Electric Field. To examine the effect of the choice of basis set shown in Table 1, we used 4-chloro-benzonitrile. We also used this compound for further examination of the Stark effect, since similar IR probes has been used recently.[9] Figure 2 shows the effect of electric field on the stretching mode, namely, ν_{CN}, which involves the motion of CN moiety in 4-chloro-benzonitrile. It is seen that the effect of the electric field is nonlinear. A probe placed in different parts of any protein would experience different magnitude fields, F_{matrix}. When the relation ν vs F is nonlinear, the local electric field may place the molecular group on more or less sensitive parts of the Stark tuning curve, as indicated schematically on the figure. Moreover, the F_{matrix} could cause the relaxed molecule to be in the region where the electric field has a very small effect in the frequency. In this case, the VSE measurements would give little information. This situation is shown in the region between the dotted lines in Figure 2. We found a maximum in the frequency-field dependence for 4-chloro-benzonitrile. There is also a minimum in the extinction coefficient in this region. In consequence, the detection of the ν_{CN} signal will be difficult. The relative extinction coefficient rises when the electric field produces a large effect in shifting the frequency. This relationship may prove valuable experimentally, where one is able to measure the extinction coefficient and the frequency.

Figure 3 shows the change of the Mulliken charges, q_C and q_N, on CN moiety of 4-chloro-benzonitrile for the same electric fields used in the Figure 2. The q_C or q_N has a quasilinear change with the electric field. Therefore, from the results in Figure 2, it follows that the relation $q_C + q_N$ vs ν_{CN} is nonlinear. This result is different from the linear relation for the dipole moment that Franzen[37] found in a model of CO adducted in heme.

Field-Dependent Frequency and Geometries of Fe Adducts in Hemes and Heme Models. Field-dependent vibrational properties of −CO, −CN, and $-NO^+$ bound to heme via an Fe ligation were examined using the same basic approach as for the small molecules.

CO in Proteins. CO competes with, and mimics, oxygen binding to Fe^{2+} in hemoproteins. Like O_2, CO does not bind to Fe^{3+} hemoproteins. The CO complexes of heme proteins have

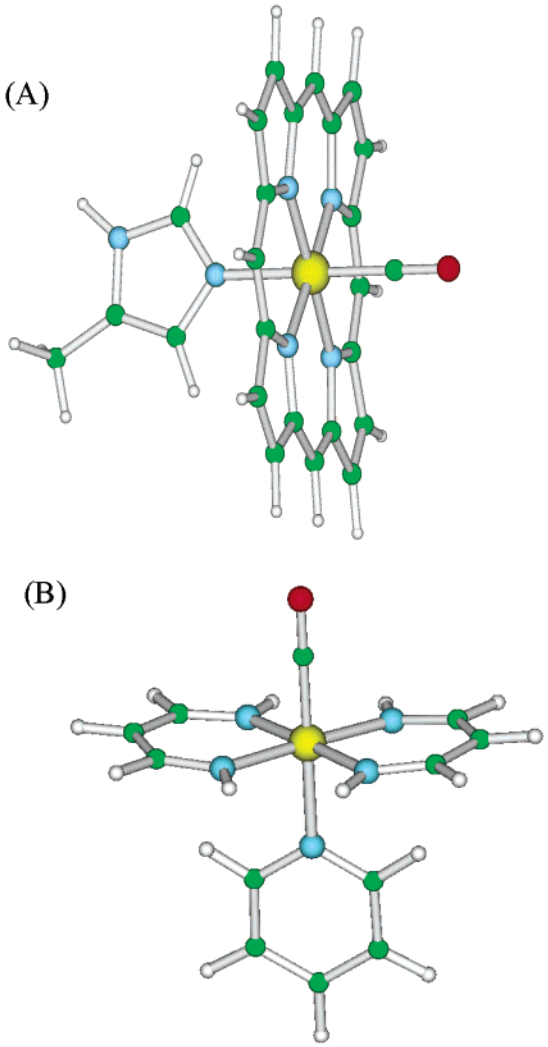

Figure 1. Clusters used to study the effect of the electric field in the stretching frequency of −CO and −CN. (A) Fe−porphine−CO/NO+. (B) Fe−$N_{pyridine}$−CO/CN.

been studied in detail by IR and Raman techniques, so there is a great deal of experimental data to compare with computations.

The total energy of the cluster changes with the amplitude of the CO stretching vibration. This is shown in Figure 4 for CO of the Fe−$N_{pyridine}$−CO cluster. The figure also illustrates that the shape of the potential curve changes when a field of $F = 0.01$ au is applied. The arrows indicate that the equilibrium position of the CO adducts also changes with applied field. The figure defines the value $\Delta E_F = 0.0336$ au (21 kcal/mol), the change in energy due to the electric field evaluated at the equilibrium position. The change in the equilibrium distance d_{CO} due to the applied electric field is ∼0.063 Å. These changes result in a Stark shift of 1.2×10^{-3} Å/(MV/cm).

The bond lengths d_{Fe-CO} and d_{C-O} or d_{C-N} for different electric fields for two different heme CO models are shown in Figure 5 (top). The arrows indicate the equilibrium distance with the electric field off. As is well established from IR and Raman experiments, as the d_{Fe-C} distance decreases, the d_{C-O} distance increases. The change in d_{Fe-CO} and d_{CO} for a positive or negative electric field is similar for the clusters used. The equilibrium distances for $F = 0$ are similar to other works.[32,37−39] The slope $d_{Fe-CO}/d_{CO}|_{eq}$ evaluated at the equilibrium distance with $F = 0$ is 10% lower for all the clusters when the frequency was calculated with the basis 6-31G than with TZV. The dotted line is the slope of $d_{Fe-CN}/d_{CN}|_{eq}$ for comparison. Figure 5

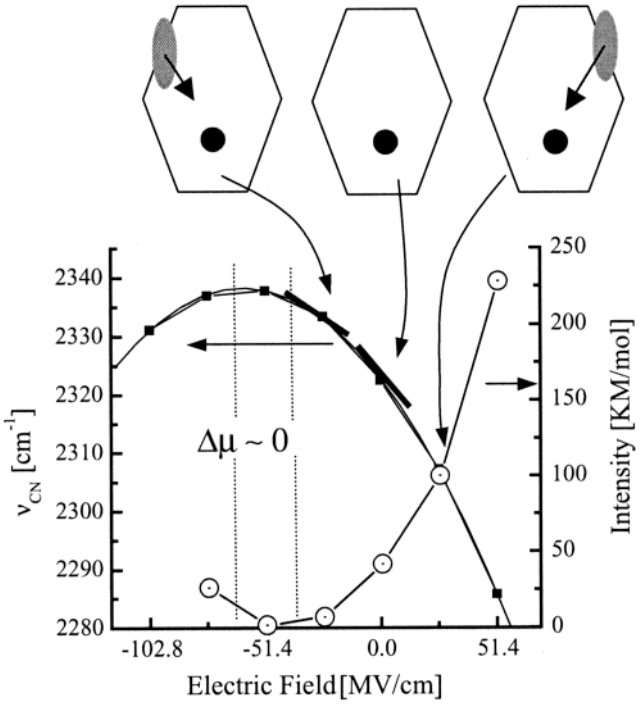

Figure 2. The frequency ν_{CN} and absorbance of CN against electric field for 4-chloro-benzonitrile. The hexagon represents a protein in wild type (center) and two different mutations. The arrow inside the hexagon represents the matrix electric field.

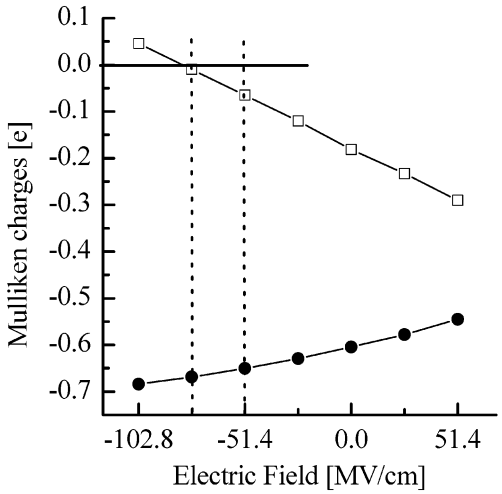

Figure 3. Mulliken charges as a function of the applied electric field on the CN moiety for 4-chloro-benzonitrile. (□) Q_N and (●) Q_C.

(bottom) shows the equilibrium distance d_{Fe-CN} vs d_{CN} for different electric fields for ferrous and ferric iron in clusters that model the heme. The arrows indicate the equilibrium distance with the electric field off. The slope $d_{Fe-CN}/d_{CN}|_{eq}$ evaluated at the equilibrium distance with the electric field off for ferric −CN is four times greater than for ferrous −CN. The change in d_{Fe-CN} and d_{CN} for a positive electric field in the ferric −CN is ∼2 times greater than for a negative electric field, indicating important asymmetry distances vs electric field. For the ferrous −CN, this asymmetry is small. The dotted line is the slope of $d_{Fe-CO}/d_{CO}|_{eq}$ for comparison.

The CO stretching frequency as a function of electric field is shown in Figure 6 (top). The effect of the electric field was linear over the range studied, and the slopes were nearly parallel for different clusters, functionals, and basis sets. The tuning rate for the Fe−$N_{pyridine}$−CO is given in Table 3. It is important to

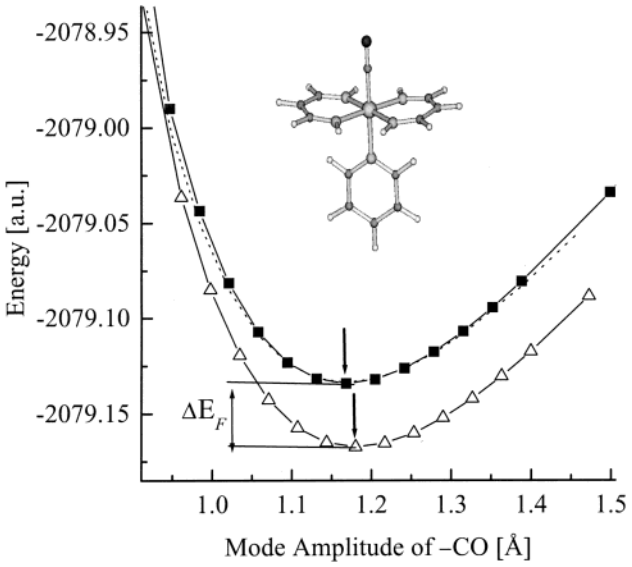

Figure 4. Energy as a function of distance for C−O in its stretching mode of vibration. See text for details. The step is ∼0.005 A. ΔE_F is the change of energy due to the electric field; the arrows indicate the equilibrium CO distance after relaxation with and without electric field. The applied field illustrated was 0.01 au. The inset shows the model used in this study.

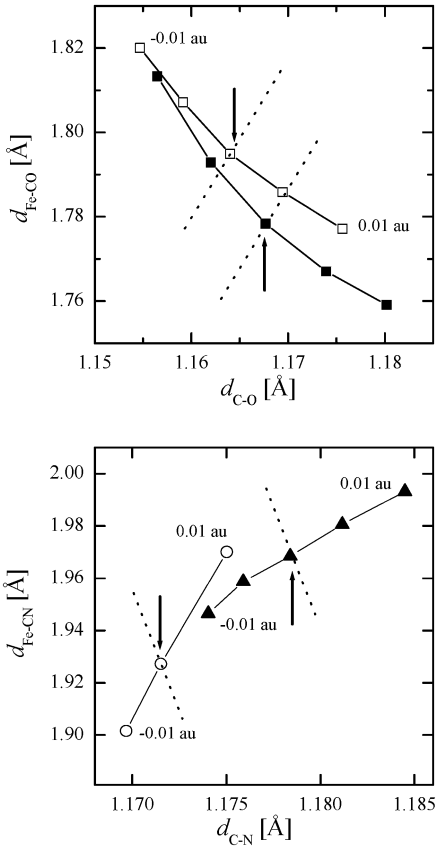

Figure 5. (Top) d_{Fe-CO} against d_{CO} for the model Fe−porphine−CO (■) and Fe−$N_{pyridine}$−CO (□). The dotted lines indicate the slope of d_{Fe-CN} against d_{CN} for the ferrous case. (Bottom_ d_{Fe-CN} against d_{CN} for the ferrous (▲) and ferric (○) model Fe−$N_{pyridine}$−CN. The dotted lines indicate the slope of d_{Fe-CO} against d_{CO} for comparison. The arrows in both figures indicate the equilibrium distance with the electric field off.

note that the use of different clusters, functionals, and basis sets gives nearly the same $\Delta\mu_{CO}$. The use of the combination B3LYP with the basis TZV in the Fe−porphine−CO model needed 6

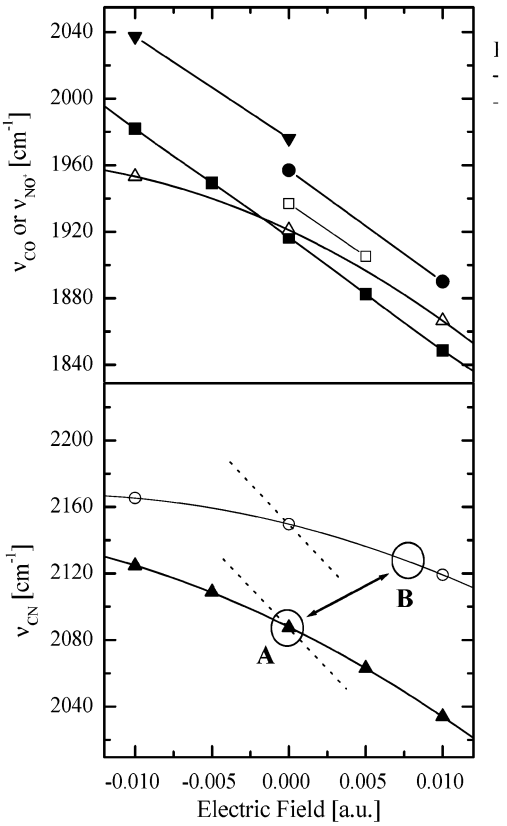

Figure 6. Effect of external field on the stretching frequencies for the −CN and −CO bond in complexes with iron. (Top) ν_{CO} and ν_{NO+} frequency for the models Fe−porphine−CO (▲, B3LYP/6-31G; □, B3LYP/TZV), Fe−porphine−NO^+ (△, B3LYP/631G), and Fe−$N_{pyridine}$−CO (■, B3LYP/TZV; ●, PW91/TZV). (Bottom) Ferrous (▲) and ferric (○) CN stretching frequencies of model Fe−$N_{pyridine}$−CN. Dotted lines indicate the slope of ν_{CO} for comparison. The big open circles indicate the change in the background electric field due to Fe^{2+} and Fe^{3+}.

times more computational time than with the basis 6-31G, although the values of $\Delta\mu$ differ by less than ∼10%. However the use of the functional Xα-LYP gave more method-dependent results, with a tuning rate of $\Delta\mu = 0.84$ cm^{-1}/MV/cm with the basis 6-31G and $\Delta\mu = 1.1$ cm^{-1}/MV/cm with the basis TZV. Together these results enabled us to establish for subsequent protein calculations the minimal computational set that would give robust results.

The main factor in the different $\Delta\mu$ between free CO or carbonyl molecules and adducted in heme proteins is the change in the population of π^* and σ orbitals of CO and the energy position of *d* orbitals of Fe.[40,41] Therefore, the effect of the electric field on the orbitals is of interest. One way of analyzing the binding mechanism and estimating the role of hybridization between the various orbitals is to carry out a population analysis based on the electronic structure calculation. Table 4 presents a population analysis of CO bonding on iron for the porphyrin−CO cluster. The values in brackets are from ref 42. As in the case of CO on top of the Fe in a finite cluster model, a decrease of the electron population of C(2s) and C(p_z) indicates that in our heme−CO model there is σ donation. The $2p_x$ and $2p_y$ orbitals of C and O increase its population showing a back donation of the iron to the π^* orbitals of the CO adducted.

Use of Mulliken Charges. Franzen used Mulliken charges to calculate the Stark tuning rate.[37] The magnitude of the charge displacement from the iron to CO can be correlated with the shift in the stretching frequency of CO. A linear correlation

TABLE 4: Population Analysis of CO Bonded to Fe in HRP Porphyrin−CO Models at Electric Field Values of −0.01, 0, and 0.01 au.[a]

	−0.01 au.	0.0 au.	0.01 au.
		C	
2s	1.47	1.50 (1.52)	1.52
2p	$p_\sigma = 0.87$	$p_\sigma = 0.86$ (0.87)	$p_\sigma = 0.87$
	$p_\pi = 1.38$	$p_\pi = 1.38$ (1.43)	$p_\pi = 1.37$
		O	
2s	1.96	1.94 (1.74)	1.92
2p	$p_\sigma = 1.31$	$p_\sigma = 1.33$ (1.38)	$p_\sigma = 1.35$
	$p_\pi = 2.93$	$p_\pi = 2.99$ (3.01)	$p_\pi = 3.07$

[a] Numbers in brackets are from ref 42.

between ν_{CO} and d_{CO} or the Mulliken charges, q_C and q_O, was proposed in ref 37, the relevant eqs 1 and 2 of which we reproduce here

$$\nu_{CO} = 2168 - 8677(d_{CO} - d_{CO}^{0}) \quad (1)$$

and

$$\nu_{CO} = 2094 + 1535(q_C + q_O) \quad (2)$$

where the frequency is in units of cm^{-1} in both equations. These equations were proposed based on over 70 vibrational frequency calculations of different model geometries and hydrogen-bonding groups.

The tuning rates of CO adducted to heme models computed in this way are 2.6 and 2.25 cm^{-1}/MV/cm using eqs 1 and 2, respectively. The result is therefore in excellent agreement with the experimental data (2.4 cm^{-1}/MV/cm). We used the charges derived from our calculations, and the result is 2.6 cm^{-1}/MV/cm using eq 2.

NO^+ Free and Adducted in Proteins. Nitric oxide reacts with both ferric and ferrous hemoproteins. The measured tuning rate is $2.0/f$ cm^{-1}/MV/cm for NO adducted to Fe in different mutants of myoglobin or for picket fence model compounds.[43] The Fe−C−O bond is linear, while Fe−N−O is bent because the extra electron. The IR spectral peak position of ν_{NO} in wild-type Mb is around 1615 cm^{-1}, for V68N−Mb−NO mutant ν_{NO} = 1581 cm^{-1}, and for H64V/V68T−Mb−NO mutant ν_{NO} = 1631 cm^{-1}.[43] We studied both the NO and NO^+ species adducted to the heme model. The NO species has a spin of 1, and calculations did not converge properly in the presence of an applied field. This problem was independent of the method and basis-set choice. Unfortunately, this is the compound for which experimental data is available.[10] We thus restricted ourselves to the case of Fe−NO^+. This adduct is isoelectric with Fe−CO and hopefully will serve as a starting point for future studies with NO. The stretching frequency as a function of the electric field is shown in Figure 6 (top). The −NO^+ adducts have a nonlinear frequency-field dependence. The bent angle of the bond Fe−N−O^+ is zero, when F is 0 or negative (Fe ← N ← O) similar to −CO, but when the electric field is applied in the positive direction (Fe → N → O), the bent angle Fe−N−O is ∼171° and the tilt is ∼5°. Recently multiple Fe−NO conformations were observed in Nitrophorin 4, and a theoretical study showed the importance of the population of bonding and antibonding orbitals of NO as responsible for the big bent and tilting angles.[44] Even though NO^+ has one electron less than −NO the bent angle observed indicates the change in the population of NO orbitals. In this case, for the calculations, we used the bigger cluster with the small 6−31 G basis set.

CN Bound to Ferrous and Ferric Heme Proteins and Nitrile. Unlike CO, which binds only to the ferrous heme, −CN can bind to both ferrous and ferric heme proteins, although the binding to ferric heme is much stronger than to ferrous heme. For ferric horse metmyoglobin−CN, the stretching frequency is centered at 2126 cm^{-1}. In human hemoglobin−CN (Hb−CN), the band is at 2122 cm^{-1} and the difference between conformers is Δ^{conf} = 11 cm^{-1}.[45] When −CN binds to the ferrous myoglobin or horseradish peroxidase (HRP), the IR frequencies are 2057 and 2029 cm^{-1}, respectively.[46] For myoglobin there may be more than one conformer with a span Δ^{conf} = 15 cm^{-1} between conformers.[47] The conformers were interpreted as an indication of polar and steric interactions in the environment of C−N group.

For the heme cluster models, Figure 6 shows the frequency against an external field for −CO and its isoelectronic counterpart −NO^+ for different functionals and basis sets (top panel) and for −CN, (bottom panel). For the CN case, by use of the model Fe−$N_{pyridine}$−CN, we calculated the electric field at the C−N moiety when Fe is either ferrous or ferric. The difference in the electric field between oxidation states is ∼43 MV/cm for N and ∼31 MV/cm for C with a mean value of ∼37 MV/cm. Thus the offset in electric field is ∼37 MV/cm more positive for ferric than for ferrous. This causes a shift in frequency independent of any protein matrix or externally applied field. This is illustrated in Figure 6, lower panel. Starting with Fe^{3+}, the zero applied field point is indicted by the circle A after a reduction to Fe^{2+} the zero point field moves to circle B on the upper, reduced, curve. The ν_{CN} frequency for the ferric −CN is less sensitive to changes in the electric field than ferric −CN. The slope $\Delta\mu^{CN} = \lim_{F\to 0} \Delta\nu_{CN}/\Delta F$ or tuning rate in the limit when F goes to zero is given in Table 3, where the tuning rates for ferric and ferrous are $\Delta\mu^{ferric}_{CN}$ and $\Delta\mu^{ferrous}_{CN}$, respectively.

Discussion

The computations described in this paper were done with the ultimate view of understanding vibrational spectral features of groups in proteins. The variation of the frequency with the electric field is a local property. The work addresses these concerns: is the effect linear with field and is the effect symmetrical around the bond? How can these features be utilized to study proteins?

IR Probes for Electric Fields in Proteins. One finding of this work is the observation that the field dependence of the stretching frequency of −CO adducted to Fe is linear within the range of electric fields used. It was also independent of the model used (Figure 6 top). A consequence of this was manifest in the vibrational Stark experiment of Boxer and collaborators for myoglobin−CO (Mb−CO). As was mentioned in the Introduction, between the mutants V68N−Mb−CO and H64V/V68T−Mb−CO, the CO molecule feels a change in the internal electric field, $F_{matrix} = f$ 26 MV/cm. However, the measured or calculated $\Delta\mu$ is the same: 2.4 cm^{-1}/(MV/cm) in the wild type and in the mutants. The tuning rate of CO bound to HRP is similar to Mb−CO (private communication, S. Boxer), indicating that the interaction of CO with Fe−porphyrin is the main factor. The VSE has been measured for the vibration of CO adducted to heme iron in myoglobin (Mb) at different pHs and for several mutants, giving a Stark tuning rate of $2.4/f$ cm^{-1}/MV/cm, four times greater than for free CO.[48] For example, the CO frequency of the V68N−Mb−CO mutant is ν_{CO} = 1922 cm^{-1} and for the H64V/V68T−Mb−CO mutant is ν_{CO} = 1984 cm^{-1}, which corresponds to a change in the internal electric field, F_{matrix}, of $\sim f$ 26 MV/cm. In the wild-type Mb−CO, a

change in the pH has been associated with a shift of $\sim$20 cm^{-1} which corresponds to a change of $\sim f$ 8 MV/cm. In contrast to small carbonyl molecules such as acetone and methylvinyl ketone, which have tuning rates similar to free CO, the tuning rate for CO−heme is higher. Overall, these results confirm the usefulness of CO as a Stark probe and the relative ease of the interpretation of frequency shifts in terms of local electrostatic fields.

Table 3 summarizes the results for the heme cluster models. The data show that $\Delta\mu^{\text{ferric}}{}_{\text{CN}}$ is half that of ferrous $\Delta\mu^{\text{ferrous}}{}_{\text{CN}}$ (Figure 6, bottom). The value for $\Delta\mu$ of free CN$^-$ is significantly smaller than for free CO. When these two groups are liganded to the heme, $\Delta\mu$ for CN increases more than for CO, probably because the CN bonding is largely ionic while CO has a covalent σ and π bond. The consequence is that their Stark tuning parameters as heme adducts are more similar. We note that despite the importance of adducted −CN as a Stark probe, the tuning rate has not been experimentally determined yet.

From these results, we can anticipate that the rather simple Stark behavior of the tuning rate seen in CO derivatives will not occur for −CN adducted to ferrous or ferric heme proteins. Indeed, it will not also occur, for example, if the compounds 4-chloro-benzonitrile or 1,4-dicyano-2-butene are used to sense the matrix electric field. In these cases, the Stark effect needs a second correction. The scheme given in Figure 2 illustrates these ideas. When there is a nonlinear relationship in ν vs F, as in the case of 4-chloro-benzonitrile, it is possible that the electric field may have a very small effect on the frequency. The same can be true when the F_{matrix} causes the relaxed molecule to be in the region where the molecule becomes relatively field insensitive. This situation is shown in the region between dotted lines in Figure 2. We found a maximum in the frequency-field dependence for 4-chloro-benzonitrile. If 4-chloro-benzonitrile is used inside a protein, in the region between dotted lines, a change in the field gives a decrease in ν_{CN} frequency. The tuning rate in the maximum gives a very small tuning rate value. Either situation would complicate the use of that group as a Stark probe.

In terms of application of the Stark tuning effects to proteins, the nitrile-labeled amino acids can be incorporated in different places in the sequence of a protein. Then with vibrational Stark spectroscopy techniques of Boxer et al. (cf. above) and quantum mechanical calculations of the type presented here, it is possible to map the electrostatic field around the probes.

The other probe that was examined is NO. There are less data available for this. The Stark effect is predicted to be less strong than for CO, and also it is not linear over the range examined (Figure 6).

The calculated tuning rate was close for small molecules for all calculation methods. At this time, we do not understand why the calculated tuning rate is in close agreement with the experiment for small molecules and relatively far for CO adducted to Fe in heme models. The use of different functionals or basis sets does not seem to be the way to improve the agreement. For calculation of the stretching frequency of CO, the use of Mulliken charges, as described out by Franzen, gave values close to the experimental values. It was farther away using the DFT methods. Thus we speculate that the reason for the tuning rate discrepancies in heme clusters could either be the model clusters used or the DFT method. Nevertheless, the approach seems to be promising, but further work will be necessary to improve agreement with experiment.

In summary, the effects of the electric field in the porphine model with −CO, −CN, and −NO$^+$ adducts and in small carbonyl and nitrile molecules were studied with DFT. We showed the importance of theoretical studies in better understanding the experimental findings.

Acknowledgment. The National Institute of Health Grant PO1 GM48310 supported this work.

References and Notes

(1) Stubner, M.; Hecht, C.; Friedrich, J. *Biophys. J.* **2002**, *83*, 3553.
(2) Stubner, M.; Hecht, C.; Friedrich, J. *J. Phys. Chem Chem Phys.* **2002**, *4*, 6080.
(3) Pal, S. K.; Peon, J.; Zewail, A. H. *Proc. Natl. Acad. Sci. U. S. A.* **2002**, *99*, 1763.
(4) Anni, H.; Vanderkooi, J. M.; Sharp, K. A.; Yonetani, T.; Hopkins, S. C.; Herenyi, L.; Fidy, J. *Biochemistry* **1994**, *33*, 3475.
(5) Manas, E. S.; Wright, W. W.; Sharp, K. A.; Friedrich, J.; Vanderkooi, J. M. *J. Phys. Chem. B* **2000**, *104*, 6932.
(6) Prabhu, N. V.; Dalosto, S. D.; Sharp, K. A.; Wright, W. W.; Vanderkooi, J. M. *J. Phys. Chem. B* **2002**, *106*, 5561.
(7) Rasnik, I.; Sharp, K.; Fee, J. A.; Vanderkooi, J. M. *J. Phys. Chem. B* **2001**, *105*, 282.
(8) Cohen, B. E.; McAnaney, T. B.; Park, E. S.; Jan, Y. N.; Boxer, S. G.; Jan, L. Y. *Science* **2002**, *296*, 1700.
(9) Getahun, Z.; Huang, C. Y.; Wang, T.; De Leon, B.; Degrado, W. F.; Gai, F. *J. Am. Chem. Soc.* **2003**, *125*, 405.
(10) Bublitz, G. U.; Boxer, S. G. *Annu. Rev. Phys. Chem.* **1997**, *48*, 213.
(11) Park, E. S.; Boxer, S. G. *J. Phys. Chem. B* **2002**, *106*, 5800.
(12) Andrews, S. S.; Boxer, S. G. *J. Phys. Chem. A* **2000**, *104*, 11853.
(13) Andrews, S. S.; Boxer, S. G. *J. Phys. Chem. A* **2002**, *106*, 469.
(14) Chattopadhyay, A.; Boxer, S. G. *J. Am. Chem. Soc.* **1995**, *117*, 1449.
(15) Reimers, J. R.; Hush, N. S. *J. Phys. Chem. A* **1999**, *103*, 10580.
(16) Thomas, M. R.; Brown D.; Franzen S.; Boxer, S. G. *Biochemistry* **2001**, *40*, 15047.
(17) Liptay, W. *Excited States* **1974**, *1*, 129.
(18) Bishop, D. M. *Rev. Mod. Phys.* **1990**, *62*, 343.
(19) Bauschlicher, C. W., Jr. *Chem. Phys. Lett.* **1985**, *118*, 307.
(20) Martí, J.; Luis, J. M.; Duran, M. *Mol. Phys.* **2000**, *98*, 513.
(21) Hush, N. S.; Reimers, J. R. *J. Phys. Chem.* **1995**, *99*, 15798.
(22) Lambert, D. K. *J. Chem. Phys.* **1988**, *89*, 3847.
(23) Lambert, D. K. *J. Chem. Phys.* **1991**, *94*, 6237.
(24) (a) Bishop, D. M. *J. Chem. Phys.* **1993**, *98*, 3179. (b) Bishop, D. M. *J. Chem. Phys.* **1993**, *99*, 4875.
(25) Brewer, S. H.; Franzen, S. *J. Chem. Phys.* **2003**, *119*, 851.
(26) Becke, A. D. *Phys. Rev. A* **1988**, *38*, 3098.
(27) Becke, A. D. *J. Chem. Phys.* **1993**, *98*, 5648.
(28) Becke, A. D. *J. Chem. Phys.* **1993**, *98*, 1372.
(29) Adamo, C.; Barone, V. *J. Chem. Phys.* **1998**, *108*, 664.
(30) Frisch, M. J.; Trucks, G. W.; Schlegel, H. B.; Scuseria, G. E.; Robb, M. A.; Cheeseman, J. R.; Zakrzewski, V. G.; Montgomery, J. A., Jr.; Stratmann, R. E.; Burant, J. C.; Dapprich, S.; Millam, J. M.; Daniels, A. D.; Kudin, K. N.; Strain, M. C.; Farkas, O.; Tomasi, J.; Barone, V.; Cossi, M.; Cammi, R.; Mennucci, B.; Pomelli, C.; Adamo, C.; Clifford, S.; Ochterski, J.; Petersson, G. A.; Ayala, P. Y.; Cui, Q.; Morokuma, K.; Malick, D. K.; Rabuck, A. D.; Raghavachari, K.; Foresman, J. B.; Cioslowski, J.; Ortiz, J. V.; Stefanov, B. B.; Liu, G.; Liashenko, A.; Piskorz, P.; Komaromi, I.; Gomperts, R.; Martin, R. L.; Fox, D. J.; Keith, T.; Al-Laham, M. A.; Peng, C. Y.; Nanayakkara, A.; Gonzalez, C.; Challacombe, M.; Gill, P. M. W.; Johnson, B. G.; Chen, W.; Wong, M. W.; Andres, J. L.; Head-Gordon, M.; Replogle, E. S.; Pople, J. A. *Gaussian 98*, revision E.2; Gaussian, Inc.: Pittsburgh, PA, 1998.
(31) Schaefer, A.; Huber, C.; Ahlrichs, R. *J. Chem. Phys.* **1994**, *100*, 5829.
(32) Dalosto, S. D.; Prabhu, N. V.; Vanderkooi, J. M.; Sharp, K. A. *J. Phys. Chem. B* **2003**, *107*, 1884.
(33) Ghosh, A.; Bocian, D. F. *J. Phys. Chem.* **1996**, *100*, 6363.
(34) Bottcher, C. J. F. *Theory of Electric Polarization*; Elsevier Press: Amsterdam, 1973.
(35) Reimers, J. R.; Hall, L. E. *J. Am. Chem. Soc.* **1999**, *121*, 3730.
(36) Pombeiro, A. J. L. *Inorg. Chem. Commun.* **2001**, *4*, 585.
(37) Franzen, S. *J. Am. Chem. Soc.* **2001**, *124*, 13271.
(38) Rovira, C.; Schulze, B.; Eichinger, M.; Evanseck, J. D.; Parrinello, M. *Biophys. J.* **2001**, *81*, 435.
(39) Sigfridsson, E.; Ryde, U. *J. Biol. Inorg. Chem.* **1999**, *4*, 99.
(40) Kushkuley, B.; Stavrov, S. S. *Biophys. J.* **1996**, *70*, 1214.
(41) Head-Gordon, M.; Tully, J. C. *Chem. Phys.* **1993**, *175*, 37.
(42) Nayak, S. K.; Nooijen, M.; Bernasek, S. L.; Blaha, P. *J. Phys. Chem.* **2001**, *105*, 164.
(43) Park, E. S.; Thomas, M. R.; Boxer, S. G. *J. Am. Chem. Soc.* **2000**, *122*, 12297.

(44) Wondimagegn, T.; Ghosh, A. *J. Am. Chem. Soc.* **2001**, *123*, 5680.
(45) Al-Mustafa, J. I. *Vib. Spectrosc.* **2002a**, *30*, 139.
(46) Reddy, K. S.; Yonetani, T.; Tsuneshige, A.; Chance, B.; Kushkuley, B.; Stavrov, S. S.; Vanderkooi, J. M. *Biochemistry* **1996**, *35*, 5562.
(47) Al-Mustafa, J. I. *Vib. Spectrosc.* **2002b**, *951*, 1.
(48) Park, E. S.; Andrews, S. S.; Hu, R. B.; Boxer, S. G. *J. Phys. Chem. B* **1999**, *103*, 9813.
(49) Fujii, H. *J. Am. Chem. Soc.* **2002**, *124*, 5936.